Single-shot readout of an electron spin in silicon

Andrea Morello[1*], Jarryd J. Pla[1], Floris A. Zwanenburg[1], Kok W. Chan[1], Hans Huebl[1†], Mikko Möttönen[1,3,4], Christopher D. Nugroho[1‡], Changyi Yang[2], Jessica A. van Donkelaar[2], Andrew D. C. Alves[2], David N. Jamieson[2], Christopher C. Escott[1], Lloyd C. L. Hollenberg[2], Robert G. Clark[1], and Andrew S. Dzurak[1]

[1] *Centre for Quantum Computer Technology,*
School of Electrical Engineering & Telecommunications,
University of New South Wales,
Sydney NSW 2052, Australia.

[2] *Centre for Quantum Computer Technology,*
School of Physics, University of Melbourne,
Melbourne VIC 3010, Australia.

[3] *Department of Applied Physics/COMP,*
Aalto University, P.O. Box 15100, 00078 Aalto, Finland.

[4] *Low Temperature Laboratory, Aalto University,*
P.O. Box 13500, 00078 Aalto, Finland.

arXiv:1003.2679v3 [cond-mat.mes-hall] 24 May 2010

The size of silicon transistors used in microelectronic devices is shrinking to the level where quantum effects become important[1]. While this presents a significant challenge for the further scaling of microprocessors, it provides the potential for radical innovations in the form of spin-based quantum computers[2–4] and spintronic devices[5]. An electron spin in Si can represent a well-isolated quantum bit with long coherence times[6] because of the weak spin-orbit coupling[7] and the possibility to eliminate nuclear spins from the bulk crystal[8]. However, the control of single electrons in Si has proved challenging, and has so far hindered the observation and manipulation of a single spin. Here we report the first demonstration of single-shot, time-resolved readout of an electron spin in Si. This has been performed in a device consisting of implanted phosphorus donors[9] coupled to a metal-oxide-semiconductor single-electron transistor[10,11] – compatible with current microelectronic technology. We observed a spin lifetime approaching 1 second at magnetic fields below 2 T, and achieved spin readout fidelity better than 90%. High-fidelity single-shot spin readout in Si opens the path to the development of a new generation of quantum computing and spintronic devices, built using the most important material in the semiconductor industry.

The projective, single-shot readout of a qubit is a crucial step in both circuit-based and measurement-based quantum computers[12]. For electron spins in solid state, this has only been achieved in GaAs/AlGaAs quantum dots coupled to charge detectors[13–15]. The spin readout was achieved utilizing spin-dependent tunnelling, in which the electron was displaced to a different location depending on its spin state. The charge detector, electrostatically coupled to the electron site, sensed whether the charge had been displaced, thereby determining the spin state. Here we apply a novel approach to charge sensing, where the detector is not only electrostatically coupled, but also tunnel-coupled to the electron site[11], as shown in Fig. 1a. As a charge detector we employ here the silicon single-electron transistor[10] (SET), a nonlinear nanoelectronic device consisting of a small island of electrons tunnel-coupled to source and drain reservoirs, electrostatically induced beneath an insulating SiO_2 layer. A current can flow from source to drain only when the electrochemical potential of the island assumes specific values[16], resulting in a characteristic pattern of sharp current peaks as a function of gate voltage (Fig. 1e). The shift in electrochemical potential arising from the tunnelling of a single electron from a nearby charge centre into the SET island is large enough to switch the current from zero to its maximum value. This tunnelling event becomes spin-dependent in the presence of a large magnetic field, when the spin-up state $|\uparrow\rangle$ has a higher energy than the spin-down state $|\downarrow\rangle$, by an amount larger than the thermal and electromagnetic broadening of electron states in the SET island. Therefore we perform the experiment in high magnetic fields, $B > 1$ T, and very low electron temperatures, $T_{\rm el} \approx 200$ mK.

The high effective mass and the valley degeneracy in silicon[17] require very tight confinement to isolate a single electron in a non-degenerate state. Phosphorus atoms in silicon naturally provide a sharp confining potential for their bound donor electron, with the additional advantage that the ^{31}P nuclear spin can be used as a long-lived quantum memory[18]. Therefore we have fabricated a device where P donors were implanted in a small region (90×90 nm^2) next to the SET (Fig. 1c). The P^+ ion fluence was chosen to maximize the likelihood that 3 donors are located at a distance $\sim 30 - 60$ nm from the SET island and can be tunnel-coupled to it, forming a parallel double-quantum-dot system[19]. The SET top gate and a plunger gate overlaying the P implanted area provide full electrostatic control of the hybrid double-dot.

To perform spin readout we bias the gates so as to tune the electrochemical potentials on the SET ($\mu_{\rm SET}$) and a nearby donor ($\mu_\downarrow$ and $\mu_\uparrow$ for states $|\downarrow\rangle$ and $|\uparrow\rangle$, respectively) such that the SET current, $I_{\rm SET}$, is zero when the

electron resides on the donor, while $I_{\mathrm{SET}} \neq 0$ when the donor is ionized. The readout protocol consists of three phases[13], shown in Fig. 1b. (i) A Load phase, during which an electron in an unknown spin state tunnels from the SET island to the donor, since $\mu_{\mathrm{SET}} > \mu_{\downarrow}, \mu_{\uparrow}$. The electron loading is signalled by I_{SET} dropping to zero.

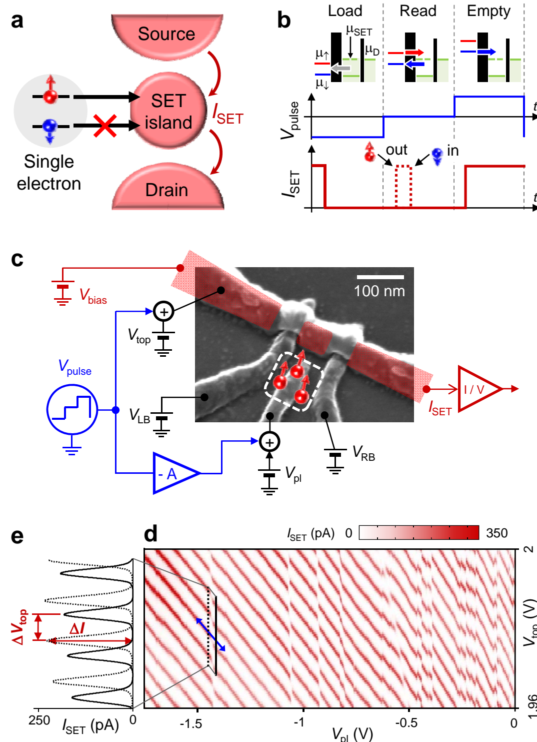

FIG. 1: **Spin readout device configuration and charge transitions.** **a** Schematic showing the spin-dependent tunnelling configuration, where a single electron can tunnel onto the island of a SET only when in a spin-up state. **b** Pulsing sequence for single-shot spin readout (see main text), and SET response, I_{SET}. The dashed peak in I_{SET} is the expected signal from a spin-up electron. The schematics at the top depict the electrochemical potentials of the electron site ($\mu_{\downarrow,\uparrow}$), of the SET island ($\mu_{\mathrm{SET}}$) and of the drain contact (μ_{D}). **c** Scanning electron micrograph of a device similar to the one measured. The P donors implant area is marked by the dashed square. The total expected number of implanted donors is 18 (Poisson statistics), of which ~ 3 are close enough to the SET to be significantly tunnel-coupled. Both DC voltages and pulses are applied to the gates as indicated. The red shaded area represents the electron layer induced by the top gate and confined beneath the SiO_2 gate oxide layer. **d** SET current I_{SET} as a function of the voltages on the top and the plunger gates, V_{top} and V_{pl}, at $B = 0$. The lines of SET Coulomb peaks are broken by charge transfer events. The blue arrow on the transition at $V_{\mathrm{pl}} \approx -1.4$ V shows the axis along which V_{top} and V_{pl} are pulsed for compensated time-resolved measurements, ensuring that μ_{SET} remains constant during the pulsing. **e** Line traces of I_{SET} along the solid and dashed lines in panel **d**. Ionizing the donor shifts the sequence of SET current peaks by an amount $\Delta V_{\mathrm{top}} = \Delta q / C_{\mathrm{top}}$, causing a change ΔI in the current. The charging energy of the SET is $E_{\mathrm{C}} \sim 1.5$ meV.

(ii) A Read phase, during which a spin-down electron remains trapped on the donor, leaving $I_{\mathrm{SET}} = 0$, but a spin-up electron can tunnel onto the SET island, causing $I_{\mathrm{SET}} = I_{\mathrm{max}}$. A (different) spin-down electron from the SET island can later tunnel back onto the donor, blocking the current again. Therefore, the signal of a state $|\uparrow\rangle$ is a single current pulse at the beginning of the Read phase. (iii) An Empty phase during which the donor is ionized, to ensure a new electron with random orientation can be loaded at the next cycle.

Measuring I_{SET} as a function of the plunger (V_{pl}) and SET top (V_{top}) gate voltages, yields the map shown in Fig. 1d. Each time a charge centre coupled to the SET changes its charge state, the sequence of SET current peaks breaks and shifts in gate voltage by an amount $\Delta V_{\mathrm{top}} = \Delta q / C_{\mathrm{top}}$, where Δq is the charge induced on the SET island and C_{top} is the capacitance between island and top gate (Fig. 1e). Figure 1d shows a large number of charge transitions for $-0.7 < V_{\mathrm{pl}} < 0$ V. Most of these transitions are irreproducible and hysteretic, and are probably caused by the charging/discharging of shallow traps at the Si/SiO_2 interface. The transitions for $V_{\mathrm{pl}} < -0.7$ V, however, are stable and well reproduced even after several thermal cycles. Their number is consistent with the expected number of implanted donors in the active area, and they have been observed in a number of similar devices[20]. Considering the results of the spin lifetime measurements discussed below, it is likely that we are observing transitions between D^+ and D^0 states[21] of implanted P donors[22].

The charge transition at $V_{\mathrm{pl}} \approx -1.4$ V in Fig. 1d has a large $\Delta q \approx 0.7e$, where $1e$ is equivalent to the spacing between adjacent current peaks. This indicates a donor very close to the SET island[11]. Accordingly, we find a fast electron tunnelling time between the donor and the SET, of order 10 μs. For comparison, the charge transition at $V_{\mathrm{pl}} \approx -1.1$ V has a lower $\Delta q \approx 0.3e$ and a much slower tunnel time $\sim$ 10 ms, consistent with a donor further away. We chose the donor transition at $V_{\mathrm{pl}} \approx -1.4$ V to implement the spin readout protocol. Figure 2b-g illustrates the method we used to find the values of V_{pulse} during the Read phase at which spin-dependent tunnelling is achieved. By lowering the Read level from too high (Fig. 2c) to too low (Fig. 2g), the time traces of I_{SET} during the Read phase show a transition from $I_{\mathrm{SET}} = I_{\mathrm{max}}$, through random telegraph signal, to $I_{\mathrm{SET}} = 0$, passing through a region where I_{SET} can be either zero (Fig. 2e) or show a spin-up signal (Fig. 2f). In this region, the condition $\mu_{\downarrow} < \mu_{\mathrm{SET}} < \mu_{\uparrow}$ is fulfilled, and a single-shot projective measurement of the electron spin state is performed. When plotting the average of several single-shot traces taken at different read levels, the correct readout range is highlighted by the appearance of a high current region at the beginning of the Read phase, spanning a time interval of the order of the electron tunnel time (see also Fig. 3c). Such a high-current region is absent in measurements performed in zero magnetic field, as expected. With a modified pulse sequence,

it is also possible to extract the Zeeman energy splitting $E_Z = g\mu_B B$ and demonstrate the deterministic loading of a $|\downarrow\rangle$ electron (see Supplementary information). Because the loading of a state $|\downarrow\rangle$ is controlled by gate voltages and occurs on $\sim 10\ \mu$s time scales as determined by the electron tunnel time, this device already realizes two essential requirements for quantum computation and quantum error correction, namely, the single-shot readout and the fast preparation of the qubit ground state[23].

For each single-shot measurement, the state is identified as $|\uparrow\rangle$ when $I_{\rm SET}$ surpasses a suitably chosen threshold $I_{\rm T}$ (Fig. 3b) during the first 100 μs of the Read phase. Defining $P_\uparrow$ as the probability to observe a spin-up electron, we find that $P_\uparrow$ decreases when increasing the wait time $\tau_{\rm w}$ before the spin is read out (Fig. 3a), because the excited state $|\uparrow\rangle$ relaxes to the ground state $|\downarrow\rangle$. The wait time dependence of $P_\uparrow$ (Fig. 3d) is well described by a single exponential decay, $P_\uparrow(\tau_{\rm w}) = P_\uparrow(0)\exp(-\tau_{\rm w}/T_1)$, where T_1 is the excited state lifetime. We note that measuring T_1 does not strictly require single-shot readout[24,25]. Since the spin-up current pulses occur with the highest probability in a well defined time interval, the average current $\langle I_{\rm SET}\rangle(t)$ has a Poissonian shape (Fig. 3c), and its integral is proportional to $P_\uparrow$. Figure 3d shows that the integral of $\langle I_{\rm SET}\rangle(t)$ for $0 < t < 100\ \mu$s can be rescaled and superimposed with $P_\uparrow$ as obtained from single-shot readout, and an exponential fit yields the same T_1 for both methods. Single-shot readout provides an absolute measure of $P_\uparrow$., but integrating $\langle I_{\rm SET}\rangle(t)$ is simpler and faster, and is used for the T_1 measurements below.

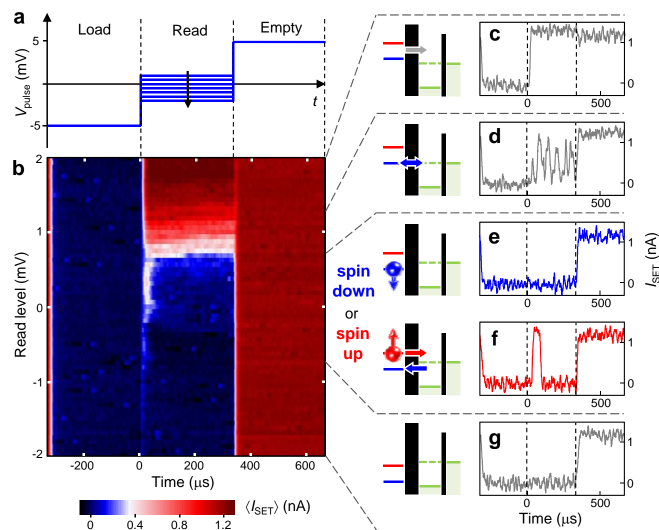

FIG. 2: **Single-shot spin readout and calibration of the read level.** **a** Three-level pulsing sequence for spin readout. The Load and Empty levels are kept constant, while the Read level is scanned from high to low. **b** SET current $I_{\rm SET}$, averaged over 128 single-shot traces, as a function of the $V_{\rm pulse}$ level during the Read phase. Data taken with an applied magnetic field $B = 5$ T and a detection bandwidth of 40 kHz (rise time 10 s). **c - g** Examples of single-shot traces. **c** Read level too high, $\mu_{\downarrow,\uparrow} > \mu_{\rm SET}$: The electron always leaves the donor during the Read pulse, regardless of its spin. **d** $\mu_\downarrow \approx \mu_{\rm SET}$: Random telegraph signal indicates an electron switching between SET island and $|\downarrow\rangle$ state. **e and f** Correct Read level, $\mu_\downarrow < \mu_{\rm SET} < \mu_\uparrow$: $I_{\rm SET} = 0$ during the Read phase indicates a $|\downarrow\rangle$ state (e). A single current pulse at the beginning of the Read phase is the signature of a $|\uparrow\rangle$ electron (f). The regime of correct Read level is recognizable by the isolated increase in $I_{\rm SET}$. **g** Read level too low, $\mu_{\downarrow,\uparrow} < \mu_{\rm SET}$: The electron never leaves the donor during the Read pulse.

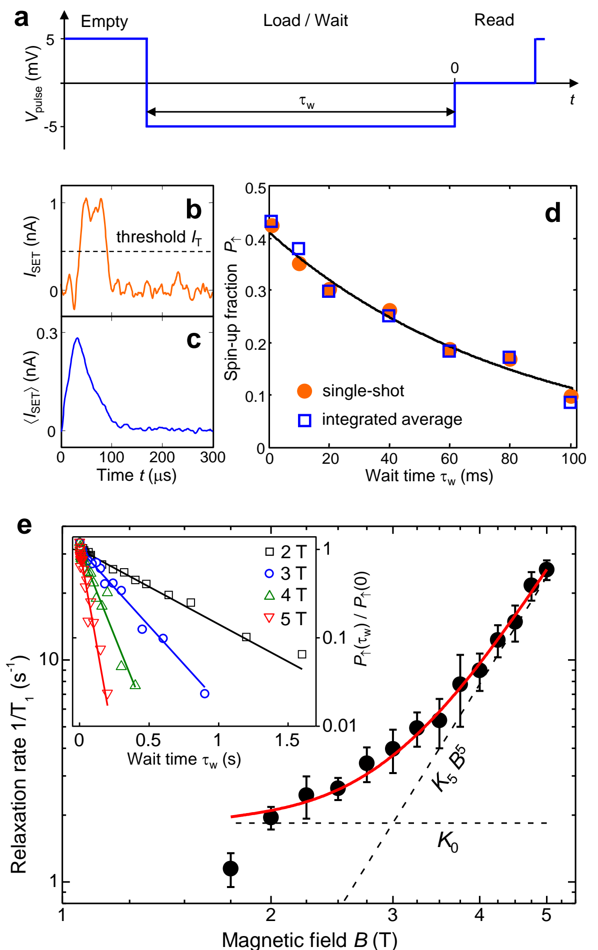

FIG. 3: **Spin-lattice relaxation rate.** **a** Pulsing sequence for measuring the spin relaxation rate $1/T_1$, identical to Fig. 2a but with a variable Load/Wait time τ_w. **b** Single-shot spin readout traces. A $|\uparrow\rangle$ state is counted when $I_{\rm SET} > I_{\rm T} = 0.45$ nA. **c** Average of 500 single-shot traces. **d** The spin-up fraction $P_\uparrow(\tau_w)$ can be obtained by counting the $|\uparrow\rangle$ states in single-shot (dots) or by integrating $\langle I_{\rm SET}\rangle(t)$ (squares). Rescaling and normalizing the integral of $\langle I_{\rm SET}\rangle$ shows that the two approaches are equivalent and can be fitted by the same exponential decay (solid line). Here $B = 5$ T. **e** Magnetic field dependence of $1/T_1$. Error bars are 95% confidence levels. The data follow $1/T_1(B) = 1.84\ {\rm s}^{-1} + 0.0076B^5\ {\rm s}^{-1}{\rm T}^{-5}$ (red line, sum of the dashed lines). The point at $B = 1.75$ T is not included in the fitted dataset. Inset: exponential decays of the normalized spin-up fraction, at different magnetic fields as indicated.

The measured spin relaxation rate as a function of magnetic field, $T_1^{-1}(B)$, at phonon temperature $T \approx 40$ mK, is plotted in Fig. 3e. The data for $B \geq 2$ T are well described by the function $T_1^{-1}(B) \approx K_0 + K_5 B^5$, with $K_0 = 1.84 \pm 0.07$ s^{-1} and $K_5 = 0.0076 \pm 0.0002$ s^{-1}T^{-5}. A fit of the form $T_1^{-1}(B) = K_0 + K_a B^a$, where K_0, K_a and a are free parameters, yields $a = 4.8 \pm 0.2$. The B^5 dependence agrees with the low-T limit[26] ($k_B T \ll g\mu_B B$) of a spin-lattice relaxation mechanism arising from the effect of spin-orbit coupling, through the deformation of the crystal lattice caused by the emission of an acoustic phonon[27] when the state $|\uparrow\rangle$ relaxes to $|\downarrow\rangle$. This result is incompatible with the known relaxation process for interface traps, which is dominated by the coupling to two-level fluctuators[28]. A recent electron spin resonance experiment on shallow traps at the Si/SiO$_2$ interface[29] found $T_1 \sim 800$ μs at $T = 350$ mK and $B = 0.32$ T, i.e. 2 to 3 orders of magnitude shorter than our result, despite the much lower magnetic field. Conversely, our measurements are in qualitative and quantitative agreement with the behaviour of T_1^{-1} measured in bulk-doped P:Si samples[7] (see Supplementary information for a detailed discussion). This constitutes a strong indication that we have measured the spin of a single electron bound to an implanted P donor.

To assess the effectiveness of the spin readout process for quantum information purposes it is important to quantify the readout fidelity, i.e., the probability that an electron spin state is recognized correctly. In Fig. 4, we show the analysis of the readout fidelity for a set of 10,000 traces. The spin state is decided based on the peak value I_p taken by $I_{SET}(t)$ in the interval $0 < t < 100$ μs. The probability distribution of the peak currents I_p is shown in Fig. 4b. The two well-resolved probability peaks indicate that I_p takes two preferential values depending on the electron spin state. We have developed a numerical model that accurately simulates the measurement process and yields two separate histograms of peak current values for the states $|\downarrow\rangle$ and $|\uparrow\rangle$, $N_{\downarrow,\uparrow}(I_p)$, respectively (see Supplementary Information). The calculated $N_{\downarrow,\uparrow}(I_p)$ are in excellent agreement with the measured histogram (Fig. 4b). With the knowledge of $N_{\downarrow,\uparrow}(I_p)$, the readout fidelities[15] are obtained as $F_\downarrow = 1 \int_{I_T}^{\infty} N_\downarrow(I)\mathrm{d}I$ and $F_\uparrow = 1 \int_{-\infty}^{I_T} N_\uparrow(I)\mathrm{d}I$ for the states $|\downarrow\rangle$ and $|\uparrow\rangle$, respectively, as a function of the discrimination threshold I_T (Fig. 4c). The integrals in $F_{\downarrow,\uparrow}$ represent the probability that the spin state is incorrectly assigned, either because a spin-down trace has a noise spike $> I_T$, or because a spin-up signal does not reach the threshold. The visibility, defined as $V = F_\downarrow + F_\uparrow - 1$, reaches a maximum value $\approx 92\%$ at $I_T = 1.1$ nA, where the readout fidelities are $F_\downarrow \approx 99\%$ and $F_\uparrow \approx 93\%$.

Combining spin resonance experiments[11,30] with the ability to read out a single spin will provide a definitive framework in which to demonstrate and exploit coherent quantum control of a donor electron and nuclear spin. The high-fidelity, single-shot electron spin readout, demonstrated here for the first time in silicon, represents the critical step to unlock the full potential of silicon-based quantum information science and technology.

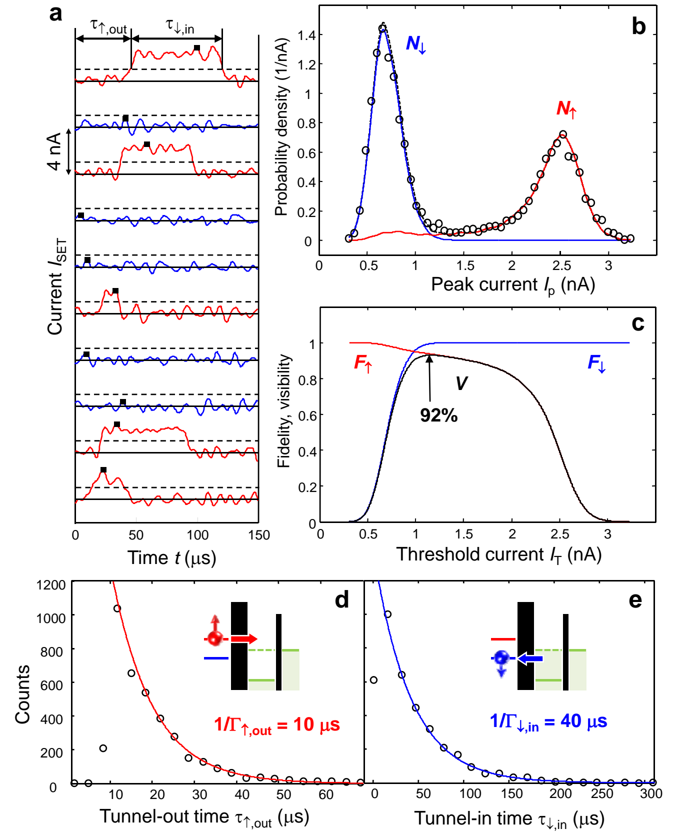

FIG. 4: **Readout fidelity and visibility.** **a** Examples of single-shot I_{SET} traces, each shifted by 4 nA for clarity, with $B = 5$ T and 120 kHz bandwidth (~ 3 μs rise/fall time). The spin is labeled $|\uparrow\rangle$ (red) or $|\downarrow\rangle$ (blue) depending on whether I_{SET} passes the threshold $I_T = 1.1$ nA (dashed lines). **b** Histogram (circles) of the maximum values of I_{SET} in the interval $0 < t < 100$ μs (black squares in panel **a**), obtained from a 10,000 shots dataset. The blue and red lines are simulated histograms for states $|\downarrow\rangle$ and $|\uparrow\rangle$, respectively, and the black dashed line is the sum of the two. The simulated curves are obtained using $P_\uparrow = 0.47$, $\Delta I = 1.9$ nA, $1/\Gamma_{\uparrow,out} = 10$ μs, $1/\Gamma_{\downarrow,in} = 40$ μs. **c** $|\downarrow\rangle$ (blue) and $|\uparrow\rangle$ (red) readout fidelities, and readout visibility (black) as a function of the discrimination threshold I_T. The maximum visibility is 92% at $I_T \approx 1.1$ nA. **d and e** Histogram (circles) of the tunnel-out times for spin-up electrons, $\tau_{\uparrow,out}$ (**d**), and subsequent tunnel-in times for spin-down electrons, $\tau_{\downarrow,in}$ (**e**), as defined on the top trace in panel **a**. In **d**, notice a systematic ~ 10 μs delay between the beginning of the Read phase and the tunnel-out events, due to the response of the amplifier and filter chain. The solid lines are exponential fits to extract the tunnel rates. These values of $1/\Gamma_{\uparrow,out}$ and $1/\Gamma_{\downarrow,in}$ were used to obtain the simulated curves in panel **b**.

Acknowledgments

We thank D.D. Awschalom, C. Tahan, J.J.L. Morton and G. Prawiroatmodjo for comments and suggestions, and R.P. Starrett, D. Barber, A. Cimmino and R. Szymanski for technical assistance. We acknowledge support from the Australian Research Council, the Australian Government, the U.S. National Security Agency and the U.S. Army Research Office under Contract No. W911NF-08-1-0527.

* Electronic address: a.morello@unsw.edu.au

† Present address: Walther-Meissner-Institut, Bayerische Akademie der Wissenschaften, 85748 Garching, Germany.

‡ Present address: Department of Physics, University of Illinois at Urbana-Champaign, Urbana IL 61801, USA.

---

[1] A. J. F. Levi. Towards quantum engineering. *Proceedings of the IEEE* **96,** 335–342 (2007).

[2] B. E. Kane. A silicon-based nuclear spin quantum computer. *Nature* **393,** 133–137 (1998).

[3] L. C. L. Hollenberg, A. D. Greentree, A. G. Fowler, and C. J. Wellard. Two-dimensional architectures for donor-based quantum computing. *Phys. Rev. B.* **74,** 045311 (2006).

[4] D. Loss and D. P. DiVincenzo. Quantum computation with quantum dots. *Phys. Rev. A* **57,** 120–126 (1998).

[5] I. Žutić, J. Fabian, and S. Das Sarma. Spintronics: Fundamentals and applications. *Rev. Mod. Phys.* **76,** 323–410 (2004).

[6] A. M. Tyryshkin, S. A. Lyon, A. V. Astashkin, and A. M. Raitsimring. Electron spin relaxation times of phosphorus donors in silicon. *Phys. Rev. B* **68,** 193207 (2003).

[7] G. Feher and E. A. Gere. Electron spin resonance experiments on donors in silicon. ii. electron spin relaxation effects. *Phys. Rev.* **114,** 1245–1256 (1959).

[8] J. W. Ager *et al.* High-purity, isotopically enriched bulk silicon. *J. Electrochem. Soc.* **152,** G448–G451 (2005).

[9] D. N. Jamieson *et al.* Controlled shallow single-ion implantation in silicon using an active substrate for sub-20-keV ions. *Appl. Phys. Lett.* **86,** 202101 (2005).

[10] S. J. Angus, A. J. Ferguson, A. S. Dzurak, and R. G. Clark. Gate-defined quantum dots in intrinsic silicon. *Nano Lett.* **7,** 2051–2055 (2007).

[11] A. Morello, C. C. Escott, H. Huebl, L. H. Willems van Beveren, L. C. L. Hollenberg, D. N. Jamieson, A. S. Dzurak, and R. G. Clark. Architecture for high-sensitivity single-shot readout and control of the electron spin of individual donors in silicon. *Phys. Rev. B* **80,** 081307(R) (2009).

[12] T. D. Ladd, F. Jelezko, R. Laflamme, Y. Nakamura, C. Monroe, and J. L. O'Brien. Quantum computers. *Nature* **464,** 45–53 (2010).

[13] J. M. Elzerman, R. Hanson, L. H. Willems van Beveren, B. Witkamp, L. M. K. Vandersypen, and L. P. Kouwenhoven. Single-shot read-out of an individual electron spin in a quantum dot. *Nature* **430,** 431–435 (2004).

[14] R. Hanson, L. H. Willems van Beveren, I. T. Vink, J. M. Elzerman, W. J. M. Naber, F. H. L. Koppens, L. P. Kouwenhoven, and L. M. K. Vandersypen. Single-shot readout of electron spin states in a quantum dot using spin-dependent tunnel rates. *Phys. Rev. Lett.* **94,** 196802 (2005).

[15] C. Barthel, D. J. Reilly, C. M. Marcus, M. P. Hanson, and A. C. Gossard. Rapid single-shot measurement of a singlet-triplet qubit. *Phys. Rev. Lett.* **103,** 160503 (2009).

[16] M. H. Devoret and R. S. Schoelkopf. Amplifying quantum signals with the single-electron transistor. *Nature* **406,** 1039–1046 (2000).

[17] S. Goswami *et al.* Controllable valley splitting in silicon quantum devices. *Nature Physics* **3,** 41–45 (2007).

[18] J. J. L. Morton *et al.* Solid-state quantum memory using the P-31 nuclear spin. *Nature*, **455,** 1085–1088 (2008).

[19] F. Hofmann, T. Heinzel, D. A. Wharam, J. P. Kotthaus, G. Böhm, W. Klein, G. Tränkle, and G. Weimann. Single electron switching in a parallel quantum dot. *Phys. Rev. B* **51,** 13872–13875 (1995).

[20] H. Huebl *et al.*. Electron tunnel rates in a donor-silicon single electron transistor hybrid. *Preprint at http://arxiv.org/abs/0905.4008* (2009).

[21] H. Sellier, G. P. Lansbergen, J. Caro, S. Rogge, N. Collaert, I. Ferain, M. Jurczak, and S. Biesemans. Transport spectroscopy of a single dopant in a gated silicon nanowire. *Phys. Rev. Lett.* **97,** 206805 (2006).

[22] K. Y. Tan *et al.* Transport spectroscopy of single phosphorus donors in a silicon nanoscale transistor. *Nano Lett.* **10,** 11–15 (2010).

[23] D. P. DiVincenzo. The physical implementation of quantum computation. *Fortschritte der Physik* **48,** 771 (2000).

[24] R. R. Hayes *et al.* Lifetime measurements (T_1) of electron spins in Si/SiGe quantum dots. *Preprint at http://arxiv.org/abs/0908.0173* (2009).

[25] M. Xiao, M. G. House, and H. W. Jiang. Measurement of the spin relaxation time of single electrons in a silicon metal-oxide-semiconductor-based quantum dot. *Phys. Rev. Lett.* **104,** 096801 (2010).

[26] R. Hanson, L. P. Kouwenhoven, J. R. Petta, S. Tarucha, and L. M. K. Vandersypen. Spins in few-electron quantum dots. *Rev. Mod. Phys.* **79,** 1217–1265 (2007).

[27] H. Hasegawa. Spin-lattice relaxation of shallow donor states in Ge and Si through a direct phonon process. *Phys. Rev.* **118,** 1523–1534 (1960).

[28] R. de Sousa. Dangling-bond spin relaxation and magnetic $1/f$ noise from the amorphous-semiconductor/oxide interface: Theory. *Phys. Rev. B* **76,** 245306 (2007).

[29] S. Shankar, A. M. Tyryshkin, J. He, and S. A. Lyon. Spin relaxation and coherence times for electrons at the Si/SiO_2 interface. *Preprint at http://arxiv.org/abs/0912.3037* (2009).

[30] M. Xiao, I. Martin, E. Yablonovitch, and H. W. Jiang. Electrical detection of the spin resonance of a single electron in a silicon field-effect transistor. *Nature* **430,** 435–439 (2004).